Modeling and Design of Buoyancy Driven Equipment for Deep Ocean Sensing

Sam Fladung[1], James Truman[2] and Anthony Westphal[3]

***Abstract*— This paper presents a view of modeling and designing buoyancy driven systems for deep ocean research. Buoyancy engines provide a method to move systems vertically within the water column and maintain depth with minimal energy. A simple dynamics simulator is presented to simulate the system and characterize its robustness to parameter variations. A test fixture and methodology is shown for characterizing hydraulic pump performance over the range of pressures and rates required for the buoyancy system.**

I. INTRODUCTION

A. Examples of buoyancy driven systems

There are many example of buoyancy driven systems in current operation. These include the APEX (Autonomous Profiling Explorer) profiling floats. These are buoyancy driven drifting sensor systems. They are capable of autonomous missions exceeding four years in length to depths of 2000m. The floats carry a variety of sensors and are used in applications ranging from ocean modeling to biogeochemical analysis. These are built around a cylindrical (either aluminum or carbon fiber) hull (Figure 1).

The APEX Deep extends this capability to 6000m of depth and can run more than 150 autonomous vertical profiles. They are built using a buoyancy engine housed within a glass sphere (Figure 2).

The Slocum Glider uses a buoyancy engine in addition to a variable pitch mechanism and rudder to allow the vehicle to navigate through the ocean. These gliders are capable of autonomous deployments of up to 18 months and can work at depths of up to 1000m (Figure 3). Systems are available using alkaline, lithium primary and rechargeable lithium ion batteries. A 3500m version is currently in development. These systems have crossed oceans as part of the Rutger's Challenger Program.[1]

II. SIMPLE DYNAMICS SIMULATOR

A simplified view of the vehicle dynamics can look at just the vertical component (ie an APEX float or standalone buoyancy engine). The free response of the system can be represented as a two variable state system. The two state variables are depth (x) and speed of change of depth ($\dot{x}$).

[1]Sam Fladung is an Electrical Engineer at Teledyne Webb Research, 49 Edgerton Dr, North Falmouth, MA 02556 sam.fladung@teledyne.com

[2]James Truman is a Hardware Engineering Manager at Teledyne Webb Research, 49 Edgerton Dr, North Falmouth, MA 02556

[3]Anthony Westphal is a Mechanical Engineer at Teledyne Benthos, 49 Edgerton Dr, North Falmouth, MA 02556

Fig. 1. Teledyne APEX Profiling Float

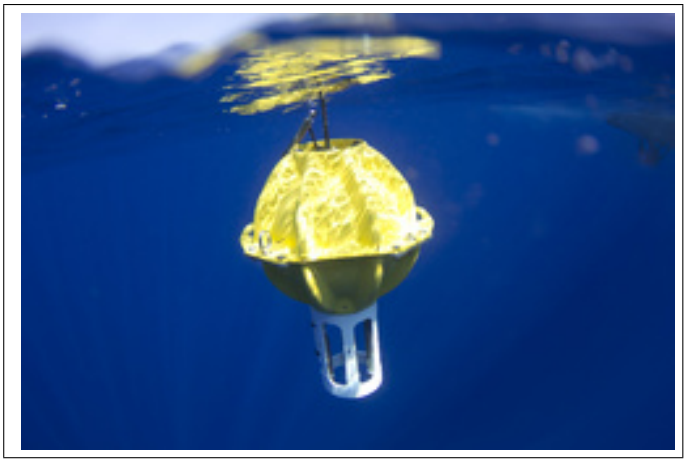

Fig. 2. Teledyne APEX Deep Profiling Float

Fig. 3. Teledyne Slocum Glider

These can be represented by a vector (X).

$$X = \begin{bmatrix} x \\ \dot{x} \end{bmatrix} \tag{1}$$

The dynamics of the system are shown in (2) (where m = system mass and $\sum F$ is the sum of all forces acting on the system:

$$\ddot{x} = \frac{\sum F}{m} \tag{2}$$

The forces acting on the system include:

- Gravity (weight)
- Buoyancy
- Drag

The gravity force is calculated in (3).

$$F_g = m * g \tag{3}$$

The equation for the magnitude of the drag force is shown in (4) with C_d as the drag coefficient and A as the cross-sectional area.

$$||F_d|| = \frac{1}{2} * \rho C_d * A * \dot{x}^2 \tag{4}$$

Note that this force must always oppose the direction of travel. Equation (5) shows the drag equation with the correct sign.

$$F_d = -\frac{1}{2} * \rho C_d * A * \dot{x}^2 * sgn(\dot{x}) \tag{5}$$

The buoyancy force is dependent on the volume of the system and the density of water at that depth/temperature. The system will compress due to both pressure and temperature. The pressure component is defined in (6) where the constant α represents the compressibility of the system in response to pressure.

$$\frac{dV}{V} = -\alpha \Delta P \tag{6}$$

The temperature component is defined in (7) where the constant β represents the change of volume in response to a temperature change.

$$\frac{dV}{V} = \beta \Delta T \tag{7}$$

These two are coupled together, although ignoring the coupling does not introduce significant error over the normal operating conditions. This removes a quadratic term and simplifies the simulation.

Equation (8) shows the combined ΔV equation.

$$\frac{dV}{V} = \beta \Delta T - \alpha \Delta P \tag{8}$$

The density of seawater is depth, temperature and salinity dependent. The density can be calculated using the UNESCO equation of state [3].

The buoyancy force calculation is shown in (9) and (10).

$$F_B = V_{sys} * \rho_{H_2O} * g \tag{9}$$

Parameter	Value
Pressure Compressibility (α)	3e-6 $\frac{1}{dBar}$
Thermal Compressibility (β)	2e-5 $\frac{1}{K}$
System Volume (V)	0.1080 m^3
System Mass (m)	113.5 kg
Area	0.0706 m^3
Drag Coefficient (C_d)	1.5

$$F_B = V_{init} * (1 - \alpha \Delta P) * (1 + \beta \Delta T) * \rho_{H_2O} * g \tag{10}$$

The system may be simulated in the discrete time domain using the formula shown in (11) and (12)

$$\dot{x}_n = \dot{x}_{n-1} + dt * \ddot{x} \tag{11}$$

$$x_n = x_{n-1} + dt * \dot{x} \tag{12}$$

This method assumes that dt is small relative to the system response. To use larger values of dt, more accurate approximations can be used to interpolate (Trapezoidal or solving the ODE in between each set of points for example (eg. using the Runge-Kutta algorithm)).

III. Example Uncontrolled Simulations

Given the equations in section II it is possible to simulate the descent of the system through the water column.

Figure 4 shows the simulated trajectory for a system with the properties shown in Table III.

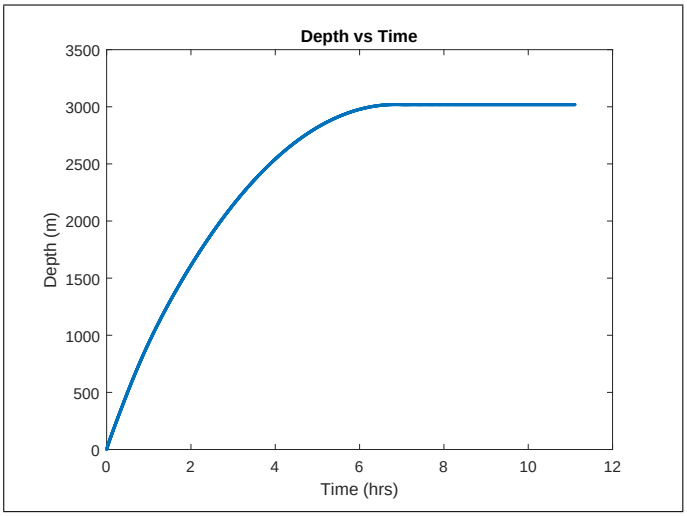

Fig. 4. Depth vs Time in Freefall With Volume Variation

It can be seen in Figure 4 that the depth stabilizes at approximately 2500m. This allows for the ballasting of a system for a specific depth. However, the system is also susceptible to errors and variation in the various parameters. Figure 5 shows the behavior with a $\pm$ 0.1 % variation in the system volume. This shows the sensitivity of buoyancy driven systems to variation in parameters. Without any buoyancy corrections, this change in volume results in a change of over 1800m in equilibrium depth. Similar effects can occur with error/variance in the compressibilities of the system, the system mass and the ocean model. The drag coefficient and

system area will change how long the system takes to reach steady state, but will not change the final depth achieved.

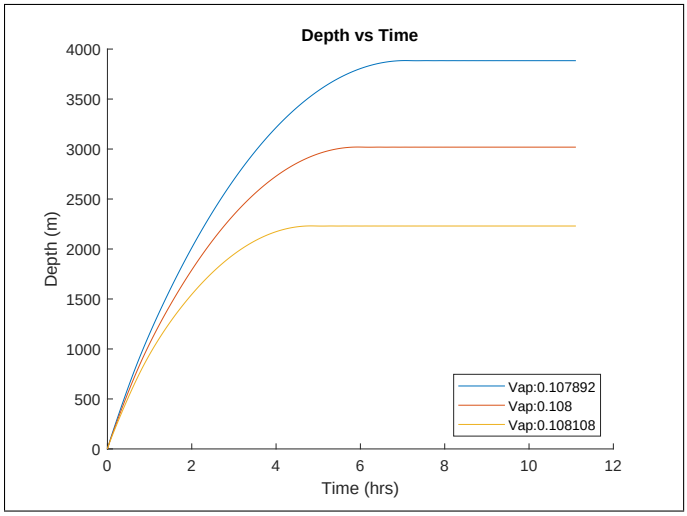

Fig. 5. Depth vs Time in Freefall

IV. Compressibility and Stability

An interesting property of these buoyancy driven systems is that as long as the system is less compressible than the seawater, it will be stable in the water column (neglecting internal waves or other water density boundaries). This can be seen from the fact that as the depth is increased, the change in the density of the system will be less than the change on the water density (based on stiffness property). This will result in an upwards buoyancy force returning the system towards its equilibrium point. Likewise, if the system is disturbed upwards, the density of the system will decrease slower than the water, giving it a downwards force to return toward its equilibrium position. This means that energy is not required for vertical adjustments to maintain the depth once equilibrium is reached.

The downside of this stability is that the greater the compressibility difference between the water and the system, the more buoyancy volume must be used to move the system by a fixed amount vertically in the water column.

V. Controlling the Buoyancy

The buoyancy of the system can be controlled by changing the systems volume. If the volume increases while the mass remains constant, the system will move upwards in the water column. This change in buoyancy can be achieved by pumping oil from inside the system into an external bladder. The size of the bladder and internal oil reservoir capacity will limit the amount of buoyancy that can be achieved by a given system.

To simulate this buoyancy control, a simple controller is implemented. The purpose of this controller is to show that the system can be controlled over the parameter variation and need not be representative of the final control algorithm.

TABLE I
Controller Parameters

Parameter	Value
PD Control P term	$0.00001\frac{m^2}{s}$
PD Control D term	$0.01m^2$
Total Oil Volume	0.0040 m^3
Oil Flow Rate Limit Out	2.5e-5 m^3/s
Oil Flow Rate Limit In	6.3e-6 m^3/s
Target Depth	2500m

TABLE II
System Parameter Variation

Parameter	Variation
Volume	$\pm 0.5\%$
Pressure Compressibility (α)	$\pm 20\%$
Coefficient of Thermal Expansion (β)	$\pm 20\%$
Drag Coefficient (C_d)	$\pm 50\%$

The controller outputs the desired oil volume rate of change (m^3/s) as shown in (13)

$$\frac{dV}{dt} = p_{term} * (x - x_{target}) + d_{term} * \dot{x} \tag{13}$$

For this simulation, we use a PD controller. The controller also enforces limits on the maximum amount of oil that can be displaced (bladder size) and the rate that the oil can move.

The controller was run with the parameters shown in Table I and the system parameters were varied by the values shown in Table II.

Figure 6 shows the depth behavior of the system with this controller. As can be readily seen, the controller now converges to the target depth in spite of the large parameter variation.

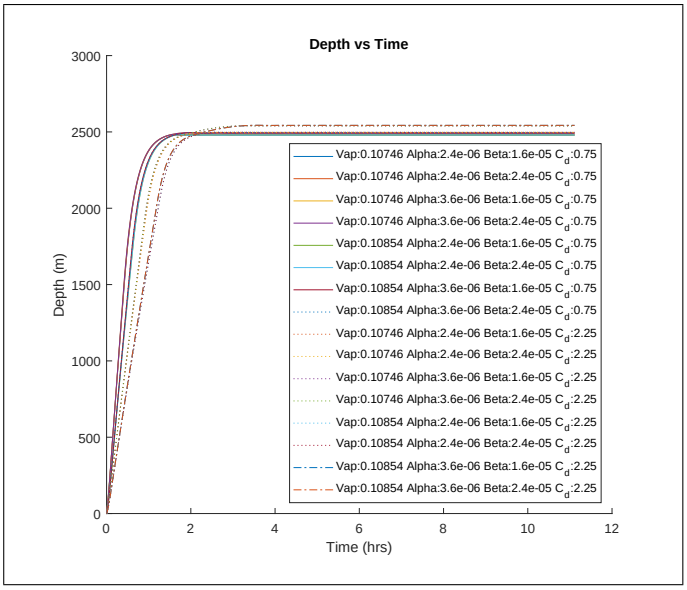

Fig. 6. Depth vs Time Under Control

VI. Buoyancy Control Energy Requirements

The energy requirements for a buoyancy system are dependent on the amount of oil flow and the depth at which it is pumped. Equation (14) shows that hydraulic work is the product of the volume of fluid moved and the pressure against which it is moved.

$$W = p * V \tag{14}$$

For a stable system (less compressible than the seawater), the energy is only needed to stop the descent or change depth. The control algorithm chosen can tradeoff energy use for system descent speed. Essentially, the earlier oil is pumped out to slow the system, the less energy it uses, but the longer it takes to reach the target depth.

A worst case energy usage can be estimated by assuming that the entire volume is pumped at the target depth. In this case, the hydraulic work required is defined in (15).

$$W_{max} = p_{target} * V_{bladder} \tag{15}$$

In addition, there will be losses in the system. See section VII for examples of the pump efficiencies.

If the controller is modelled, the simulation can give an energy use estimate. Figure 7 shows the energy used with the simple simulation controller. The energy is around half the worst case energy.

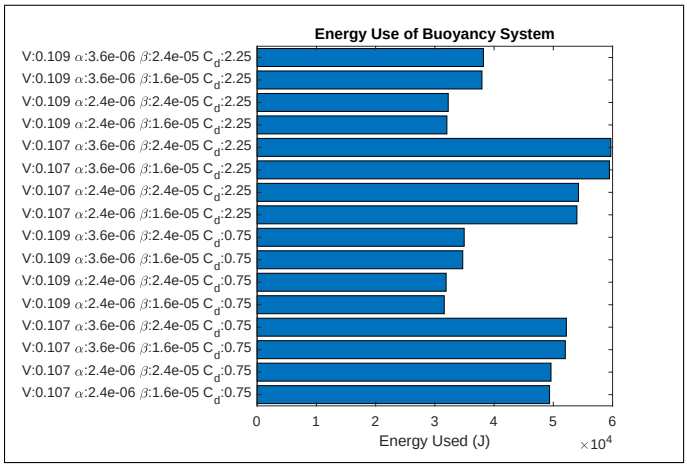

Fig. 7. Energy Used To Stabilize At Depth

VII. Buoyancy Pump Charecterizations

The pump chosen for a buoyancy system is primarily selected for pressure, pump rate, and efficiency. The pump must be able to pump against at least the ocean pressure at the maximum expected depth plus a safety factor. The pump rate determines how fast the system can change its buoyancy. A faster rate allows the system to move quicker between different depths. Efficiency determines the energy requirements for the system. In addition, there are often mechanical and electrical constraints on the size and power of the system.

A. Pump Test Setup

In order to evaluate hydraulic pumps for their suitability in specific buoyancy applications, the following test setup shown in Figure 8 was used. The fixture connects the pump between two reservoirs. The hydraulic flow is routed through an adjustable pressure relief valve to simulate the ocean pressure. The mass of the oil moved through the system is measured by a scale under the output reservoir. In order to avoid startup transient effects, the pump is brought to full speed several seconds prior to the measurements beginning. This alleviates accelleration effects. The pump and input reservoir are held in a thermal chamber at approximately 4°C as this is the expected operating range.

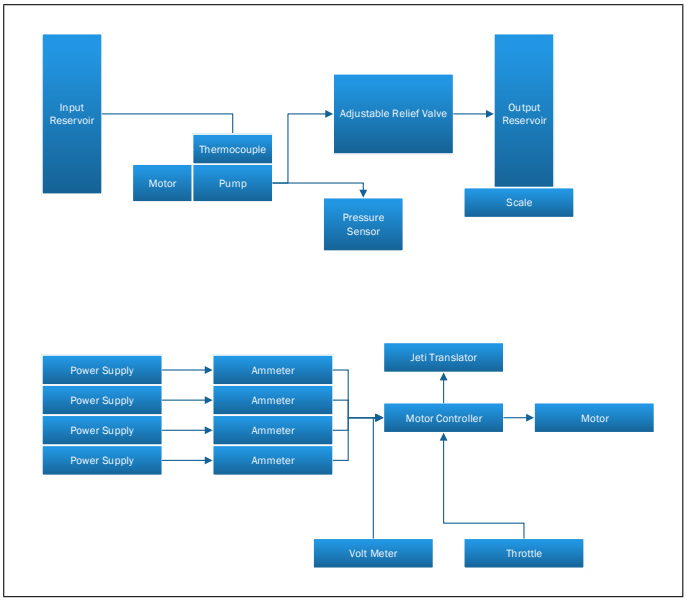

Fig. 8. Test Fixture Block Diagram for Pump Testing. Shows the hydraulic and electrical connections of the system.

To evaluate the pump the pump motor speed and relief valve pressure are used as control variables. The motor speed, output pressure, input current, input voltage and reservoir mass are measured and recorded while the system is running at steady state. Startup and stop transients are removed from the data.

B. Pump System Under Test

An example pump with measurements is included here. The pump in this example was a radial piston pump with a nominal displacement of 0.63 cc/rev.

C. Visualizing Pump Data

The system efficiency, effective displacement and power usage are calculated for each test using (16) to (20). The electrical power is calculate as

$$P_{in} = mean(I_{in} * V_{in}) \tag{16}$$

where P_{in} is the electrical power input, I_{in} represents the measured current inputs and V_{in} represents the measured voltage inputs to the motor system.

The electrical energy used is calculated as

$$U_{in} = P_{in} * \Delta t \tag{17}$$

where U_{in} is the energy used and Δt is the test time interval.

The hydraulic output work is calaculated as

$$W_{out} = mean(p) * \frac{\Delta m}{\rho_{fluid}} \tag{18}$$

where W_{out} is the output work, p is the measured pressure signal, Δm is the change in mass over the test time interval and ρ_{fluid} is the density of the fluid at the test temperature.

The efficiency (η) is calculated in (19)

$$\eta = \frac{W_{out}}{U_{in}} \tag{19}$$

The effective displacement is calculate as

$$Q_v = \frac{\Delta m}{\rho_{fluid} * \Delta t} \frac{1}{\omega_{motor}} \tag{20}$$

where Q_v is the effective displacement, and ω_{motor} is the angular speed of the motor.

These are plotted on a contour plot with intermediate values interpolated on a grid between them. This shows the expected value between actual measurements. Parts of the graph region are outside of the test region either due to exceeding the power requirements of the test setup or being below the expected operating speed of the motor. These areas appear as white in the graphs. The actual data points are overlayed on the plots as red circles to indicate the locations of measurements. Plots are shown with actual measurements for an example motor/pump combination.

Figure 9 shows the electrical power required to run the pump at the operating point (speed and pressure). The power requirement drives other system considerations including battery sizing. Depending on the application, this may limit the speed at which the pump can be run at different depths. The equipotential lines on the contour plots show the safe operating limits for a given power limitation.

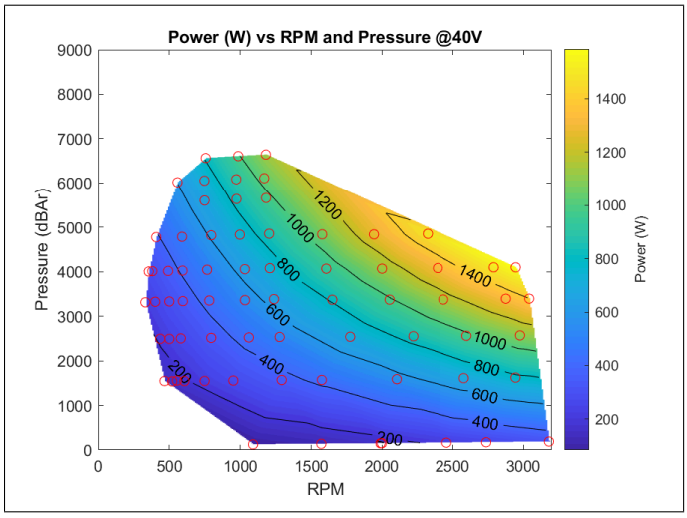

Fig. 9. Power vs RPM and Pressure For Hydraulic Pump

The mechanical efficiency plot in Figure 10 shows where the pump operates most efficiently. Unfortunately the optimal point for efficiency may lie outside of the safe operating area from a power or current perspective and so a compromise must be reached. The maximum efficiency for this pump and motor combination was shown to be around 4000dBar.

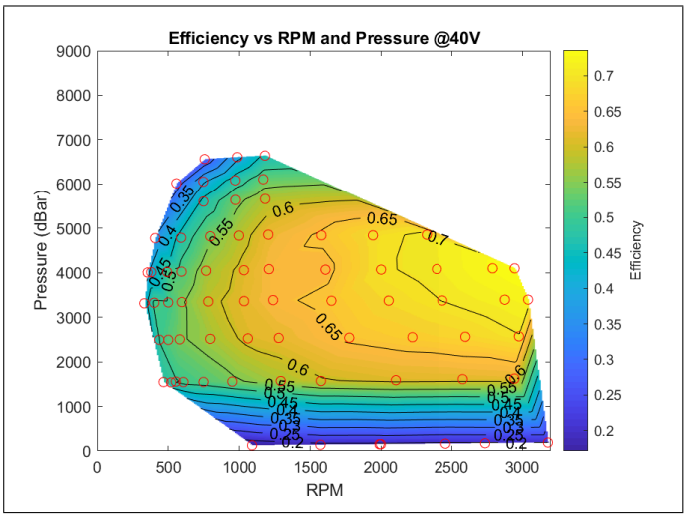

Fig. 10. Mechanical Efficiency vs RPM and Pressure For Hydraulic Pump

The final results plot is shown in Figure 11 which shows the effective displacement of the pump. This shows how much oil is moved with each rotation of the pump. This can be used to identify mismatches of oil viscosity to the pump. If there is an excessive drop in the effective displacement, the oil may have insufficient viscosity for use at the tested temperature.

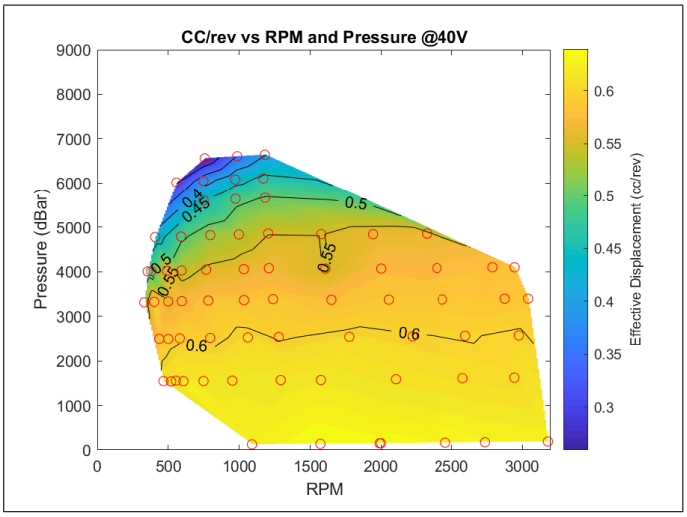

Fig. 11. Volumetric Efficiency vs RPM and Pressure For Hydraulic Pump

D. Viscosity

The hydraulic fluid used with the pump is an integral part of the system. The viscosity of the oil can have a large effect on pump performance. If the viscosity is too low,

the volumetric efficiency is reduced. If it is too high, the frictional losses in the system will become large [2]. The viscosity is a temperature-dependent parameter. This means it is important to test the system under the temperature range under which it will be operated.

VIII. CONCLUSIONS

Buoyancy engines can be used to move equipment to desired depths in the ocean. They provide the ability to adjust for parameter variation of the system. When made stiffer than the water, they require negligible energy to maintain a depth. Pumps can be sized to deliver the required buoyancy for a system and tested to verify their behavior over the operating range. Simulation and the test setup provide an effective design tool for optimizing performance.

REFERENCES

[1] Dobson, Collin, J. Mart, N. Strandskov, J. Kohut, O. Schofield, S. Glenn, C. Jones, C. Barrera. 2013. The Challenger Glider Mission: A Global Ocean Predictive Skill Experiement, Proceedings Oceans IEEE MTS 2013, San Diego.

[2] Rydberg, Karl-Erik. (2013). Hydraulic Fluid Properties and their Impact on Energy Efficiency. 447-453. 10.3384/ecp1392a44.

[3] UNESCO (1981) Tenth report of the joint panel on oceanographic tables and standards. UNESCO Technical Papers in Marine Science, Paris, 25 p